ACKNOWLEDGMENTS

We wish to thank the SLAC Operation Crew, and R. Watt and the 40-in. Bubble Chamber Group for their assistance in performing this experiment. We thank Z. G. T. Guiragossian, P. Seyboth, and G. Wolf for their help during the early stages of the experiment.

*Work supported in part by the U. S. Atomic Energy Committee.

[1] J. Ballam *et al.*, Nucl. Instrum. Methods 73, 53 (1969).

[2] Y. Eisenberg *et al.*, Phys. Rev. D 5, 15 (1972).

[3] T. H. Knasel, DESY Report No. 70/3 (unpublished).

[4] ABBHHM Collaboration, Phys. Rev. 188, 2060 (1969).

[5] M. Davier *et al.*, contributed paper to the Sixteenth International Conference on High Energy Physics National Accelerator Laboratory, Batavia, Ill., 1972 (unpublished).

[6] W. J. Podolsky, Ph.D. thesis, LBL Report No. UCRL-20128 (unpublished).

[7] Y. Eisenberg *et al.*, Nucl. Phys. B25, 499 (1971).

[8] G. Alexander *et al.*, Phys. Rev. Lett., 26, 340 (1971).

[9] M. Muirhead and A. Poppleton, Phys. Lett. 29B, 448 (1969).

[10] T. Hofmokl and A. Wroblewski, Phys. Lett. 31B, 391 (1970).

[11] J. D. Jackson, Nuovo Cimento 34, 1644 (1964).

[12] Cambridge Bubble Chamber Group, Phys. Rev. 169, 1081 (1968).

[13] Y. Eisenberg *et al.*, Phys. Rev. Lett. 22, 669 (1969).

[14] J. Ballam *et al.*, Phys. Lett. 30B, 421 (1969).

[15] See, e.g., R. Diebold, in *Proceedings of the Sixteenth International Conference on High Energy Physics, National Accelerator Laboratory, Chicago-Batavia, Ill., 1972*, edited by J. D. Jackson and A. Roberts (NAL, Batavia, Ill., 1973).

[16] Particle Data Group, Phys. Lett. 39B, 1 (1972).

[17] H. H. Bingham *et al.*, Phys. Lett. 41B, 635 (1972).

[18] C. Bacci *et al.*, Phys. Lett. 38B, 551 (1972).

[19] See, e.g., J. D. Jackson, in *Proceedings of the Fifth International Conference on Elementary Particles, Lund, 1969*, edited by G. von Dardel (Berlingska Boktryckeriet, Lund, Sweden, 1970), p. 61.

[20] G. Alexander *et al.*, Phys. Rev. 177, 2092 (1969).

[21] See, e.g., V. D. Barger and D. B. Cline, *Phenomenological Theories of High Energy Scattering* (Benjamin, New York, 1969).

Measurement of the $K^0_{\mu 3}/K^0_{e 3}$ Branching Ratio, the $K^0_{l 3}$ Form Factors, and the $K^0_{\pi 3}$ Decay Parameters*

G. W. Brandenburg, W. B. Johnson, D. W. G. S. Leith, J. S. Loos†
J. A. J. Matthews, F. C. Winkelmann,‡ and R. J. Yamartino§
Stanford Linear Accelerator Center, Stanford University, Stanford, California 94305
(Received 26 March 1973)

In a hydrogen bubble-chamber experiment with a K_L beam we have measured the $K^0_{\mu 3}/K^0_{e 3}$ branching ratio to be $R = 0.741 \pm 0.044$ and the slope of the f_+ form factor to be $\lambda_+ = 0.019 \pm 0.013$. The data have been analyzed with a new variable, $(p_T^+)^2$, which isolates a sample of unique K_{e3} decays and is independent of the K_L beam momentum. These results are compatible with the predictions of K^* dominance for f_+ and the Callan-Treiman relation for f_0, but indicate a breaking of the $\Delta I = \frac{1}{2}$ rule. We have also determined the $(K_L \to \pi^+\pi^-\pi^0)/(\text{all charged } K_L \text{ decays})$ branching ratio to be $R_\pi = 0.146 \pm 0.004$, and have found the $E^*_{\pi^0}$ slope of the $K_{\pi 3}$ Dalitz plot to be given by $g = 0.73 \pm 0.04$.

I. INTRODUCTION

In recent years there have been numerous experimental studies of the semileptonic kaon decays, $K \to \pi e \nu$ and $K \to \pi \mu \nu$.[1] One parameter which has remained in doubt, however, is the $K^0_{\mu 3}/K^0_{e 3}$ branching ratio (R). This important parameter relates the two K_{l3} form factors f_+ and f_- and its comparison with the corresponding ratio for charged-K decays is a sensitive test of the $\Delta I = \frac{1}{2}$ rule. In this paper we report a new measurement of R from a high-statistics exposure of a hydrogen bubble chamber to a K_L beam at SLAC. The bubble chamber provides bias-free geometrical acceptance in addition to good momentum resolution.

In order to extract R from the data, we have

defined a new variable $(p_T')^2$, which is independent of the incident K_L momentum and which isolates a sample of unique K_{e3} decays. In addition, the uniquely identified K_{e3} decays are used to determine the slope of the f_+ form factor (λ_+). The slope of the f_0 form factor (λ_0) is then derived from our measurements of R and λ_+ and is compared with the Callan-Treiman relation. Finally, using our data for the decay $K_L \to \pi^+ \pi^- \pi^0$, we have measured the branching ratio of charged $K_{\pi 3}$ decays to all charged K_L decays and the $K_{\pi 3}$ Dalitz plot slope parameter.

Section II contains a brief review of K_{l3} phenomenology. The experimental procedures and the kinematical separation of the decay modes are outlined in Sec. III. The measurements of λ_+ and R are described in Secs. IV and V, respectively, and these results are discussed in Sec. VI. The results on the $K_{\pi 3}$ decay mode are presented in Sec. VII.

II. PHENOMENOLOGY OF K_{l3} DECAYS

Assuming the pure vector nature of K_{l3} decays, $K \to \pi l \nu$, their transition amplitude is given by[1]

$$M \propto [(k + q)_\mu f_+(t) + (k - q)_\mu f_-(t)]$$

$$\times \bar{u}_l \gamma_\mu (1 + \gamma_5) u_\nu , \qquad (1)$$

where k and q are the four-momenta of the K and π, respectively. The form factors f_+ and f_- are real functions of t (assuming time-reversal invariance); t in turn depends only on the π energy in the K rest frame (E_π^*):

$$t = (k - q)^2 = m_K^2 + m_\pi^2 - 2 m_K E_\pi^* . \qquad (2)$$

The transition probability is then

$$W \propto A f_+^2 + B f_+ f_- + C f_-^2$$

$$\propto f_+^2 (A + B \xi + C \xi^2) , \qquad (3)$$

where A, B, and C are functions of the Dalitz plot variables and $\xi = f_-/f_+$. The terms B and C are both proportional to m_l^2; consequently only the f_+ form factor is important for K_{e3} decays. $K_{\mu 3}$ decays, on the other hand, depend on both f_+ and f_-.

The form factors are generally expanded linearly in t:

$$\begin{aligned}
f_\pm(t) &\simeq f_\pm(0)(1 + \lambda_\pm t/m_\pi^2) , \\
\xi(t) &\simeq \xi(0) + \Lambda t/m_\pi^2 , \\
\xi(0) &= f_-(0)/f_+(0) , \\
\Lambda &\simeq \xi(0)(\lambda_- - \lambda_+) .
\end{aligned} \qquad (4)$$

Since $f_+(0)$ is determined by the K_{e3} transition rate, three parameters remain to be determined to first order in t: λ_+, $\xi(0)$, and either λ_- or Λ.

Because of the relative insensitivity of the transition amplitude to f_-, only the first two parameters have been experimentally well determined, and λ_- has been found to be roughly compatible with zero.[1] We assume $\lambda_- = 0$ in the following analysis, although our results would not be affected by values of λ_- similar in magnitude to λ_+. Of the remaining parameters, λ_+ can be obtained from K_{e3} or $K_{\mu 3}$ Dalitz plot studies, while both the $K_{\mu 3}$ Dalitz plot and the μ polarization can be used to determine $\xi(0)$. Assuming μ-e universality, i.e., that f_+ is equal for K_{e3} and $K_{\mu 3}$ decays, then the integration of Eq. (3) over the Dalitz plot yields a quadratic expression for the $K_{\mu 3}^0/K_{e 3}^0$ branching ratio in terms of λ_+ and $\xi(0)$:

$$R \simeq 0.645 + 0.125\,\xi(0) + 0.019\,\xi^2(0)$$

$$+ 1.32\,\lambda_+ + 0.006\,\xi(0)\,\lambda_+ . \qquad (5)$$

From a theoretical standpoint a more useful set of form factors is obtained by replacing $f_-(t)$ with

$$f_0(t) = f_+(t) + \frac{t}{m_K^2 - m_\pi^2} f_-(t)$$

$$\simeq f_+(0)(1 + \lambda_0 t/m_\pi^2) . \qquad (6)$$

Most predictions are in terms of f_+ and f_0, which are related, respectively, to the 1^- and 0^+ amplitudes for the lepton pair. In this case the two parameters to be determined are λ_+ and λ_0, where

$$\lambda_0 = \lambda_+ + \frac{m_\pi^2}{m_K^2 - m_\pi^2}\,\xi(0) , \qquad (7)$$

and where the approximation of a linear expansion for f_0 corresponds to the assumption that $\lambda_- = 0$. An advantage of this parametrization is that the experimental determinations of λ_+ and λ_0 are in general not as highly correlated as those of λ_+ and $\xi(0)$. As an example, the branching ratio R obtained by substituting (7) into (5) is primarily a function of λ_0:

$$R \simeq 0.645 + 1.46\,\lambda_0 + 2.55\,\lambda_0^2$$

$$- 0.144\,\lambda_+ - 5.03\,\lambda_0\lambda_+ . \qquad (8)$$

In the present experiment we directly measure R and λ_+ and then obtain values for $\xi(0)$ and λ_0 using Eqs. (5) and (8), respectively.

A few examples of the many theoretical predictions for the K_{l3} form factors are as follows.[1] $K^*(890)$ dominance of the dispersion relation for f_+ predicts $\lambda_+ \simeq 0.023$. Current algebra plus partial conservation of axial-vector current (PCAC) give the Callan-Treiman relation $f_0(m_K^2) \simeq 1.27 f_0(0)$, where $t = m_K^2$ is outside the physical region. If a linear t dependence is assumed for f_0, then the latter relation implies $\lambda_0 \simeq 0.021$. Finally the $\Delta I = \frac{1}{2}$ rule for leptonic decays predicts that f_+ and f_0

for K^0 decays be exactly $\sqrt{2}$ times the corresponding form factors for K^+ decays. This in turn predicts that the $K_{\mu 3}/K_{e 3}$ branching ratios for K^0 and K^+ decays are equal, except for small (<1%) radiative and phase-space corrections. We defer the comparison of these predictions with the experimental data until Sec. VI.

III. EXPERIMENTAL PROCEDURE

A. K_L Bubble-Chamber Exposure

The data for this study came from approximately 320 000 photographs taken in the SLAC 40-in. hydrogen bubble chamber exposed to a K_L beam. These pictures are part of an 800 000 picture investigation of $K_L p$ hadronic interactions. The beam was produced by impinging a high-energy electron beam on a beryllium target 56 m upstream of the chamber,[2] and yielded approximately 25 K_L per picture. The K_L momentum spectrum, as shown in Fig. 1, peaks at about 4 GeV/c and extends to 12 GeV/c.

The sample of K_L decays has been obtained by scanning for 2-prong (V) events not associated with an interaction in the chamber.[3] No attempt has been made at the scanning stage to identify individual decay modes. These events have been measured on the SLAC spiral reader or on film plane devices and reconstructed using the program TVGP.[4] Any events which failed because of bad measurement have been remeasured. In addition to the present study of the K_L decay parameters, these data have also been used to determine the K_L momentum spectrum by a statistical method.[2]

TABLE I. Estimated contaminations and losses for the final K_L sample.

Contamination	Fraction
Nonbeam K_L decays	0.003 ± 0.002
Dalitz pairs from $K_L \to 3\pi^0$	0.002 ± 0.001
γ, K_S, Λ tails outside mass cuts	<0.001
Radiative K_S decays	<0.001
$K_L p \to K^{\pm}\pi^{\mp}p$ with invisible recoil proton	<0.001

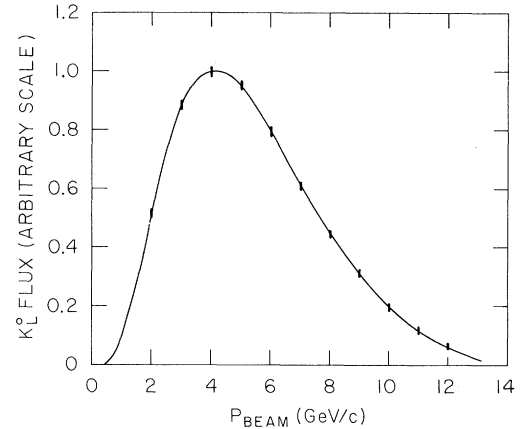| Loss	Fraction
K_{e3} with large bremsstrahlung near K_L decay vertex	0.02 ± 0.01 (of K_{e3})
Pion decays near K_L decay vertex	0.004 ± 0.002
$K_L \to \pi^+\pi^-\pi^0$ with Dalitz pairs	0.005 ± 0.002 (of $K_{\pi 3}$)
K_L decay scanned as "obvious electron pair"	<0.001

FIG. 1. Momentum spectrum of the K_L beam at the bubble chamber. The error bars represent the uncertainty in the spectrum determination (see Ref. 2).

B. Selection of K_L Decays

For an event to be selected as a K_L beam decay it must be compatible within measurement errors with any of the decay modes $\pi e \nu$, $\pi \mu \nu$, or $\pi^+\pi^-\pi^0$. However, since the beam momentum is unknown, no kinematic fitting is possible. In order to remove γ conversions and K_S and Λ decays, any events satisfying the following mass cuts have been excluded from the data:

$$M(e^+e^-) < 35 \text{ MeV} ,$$

$$485 < M(\pi^+\pi^-) < 510 \text{ MeV} ,$$

$$1110 < M(p\pi^-) < 1120 \text{ MeV},$$

where the mass assignments of the charged particles are as indicated. As estimated from the Monte Carlo calculation discussed below, these cuts also remove approximately 8% of the K_L decays. Finally, to avoid events where scanning and/or measuring biases may occur, we have required that both tracks have lab momenta greater than 50 MeV/c and that the lab opening angle be less than 45°. These cuts eliminate 2% and 5%, respectively, of the true K_L sample. None of the above cuts strongly affect the Dalitz plot distributions.

Selecting events in this manner we find no evidence of any contamination in the K_L sample above the 1% level as shown in Table I. The only significant bias remaining is an estimated $2 \pm 1\%$ loss of K_{e3} decays due to electron bremsstrahlung near the decay vertex. This is based on the assumption that electron tracks which lose more than ~15% of their energy in the first 10 cm will be unmeasurable. Other possible sources of bias, such as nonbeam K_L decays, pion decays in flight, and Dalitz pairs from $K_{\pi 3}$ decays are seen to be neg-

ligible. The final sample of K_L decays consists of
20 193 events.

C. Monte Carlo Simulation

In order to extract the K_L decay parameters
from our data, we have generated Monte Carlo
events for the three charged K_L decay modes. The
K_{l3} matrix elements discussed in Sec. II have been
modified by radiative corrections[5]; the $K_{\pi 3}$ matrix
element squared is assumed to be linear in the π^0
Dalitz plot energy (see Sec. VII) and has been cor-
rected for the Coulomb interaction of the charged
pions.[6] The events have been generated using the
beam spectrum shown in Fig. 1, after weighting
the spectrum by the decay probability. The lab
momentum vectors of both charged particles as
well as the K_L beam direction have been perturbed
by an amount corresponding to the measurement
errors in our experiment. Finally, the Monte
Carlo events have been subjected to the same
selection criteria as the data sample.

For comparison with the data the simulated
events have been transformed to the lab system
from their rest frame, where the radiative cor-
rections were applied. We note that this procedure
ensures that the kinematics of radiative decays is
correctly treated. This is in contrast with other
analyses where the observed events, which may
in fact be four-body radiative decays, are trans-
formed to their "rest frame" assuming three-body
kinematics.

The measurement errors for the charged tracks
have been parametrized as a function of momen-
tum by averaging the track errors for actual
events. These errors, which are computed by the
reconstruction program TVGP,[4] are a combination
of the setting error and the uncertainty due to
multiple scattering. To check the error paramet-
rization, we have investigated the width of the
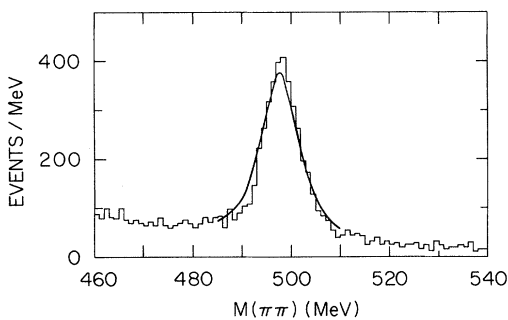$K_S \rightarrow \pi^+\pi^-$ peak shown in Fig. 2, where no K_L decay

restriction has been applied to the data. The curve
shows the Monte Carlo prediction for K_S decays
generated according to the observed K_S momentum
spectrum and normalized to the K_S peak. The
experimental mass resolution is seen to be ade-
quately reproduced by the Monte Carlo program.

In addition to the track measurement error, there
is also a small uncertainty in the direction of the
K_L beam. This results from the slight jitter of the
film position relative to the chamber and not from
the negligible size of the target, which is 56 m up-
stream. The size of this effect has been deter-
mined by plotting the missing transverse momen-
tum for the kinematically overconstrained events
of the type $K_L p \rightarrow K^+\pi^\mp p$. This is shown in Fig. 3,
where $p_y(p_z)$ is the momentum component trans-
verse to the beam and parallel (perpendicular) to
the film plane. It is found that a beam direction
uncertainty of 1 mrad (2 mrad) in the y (z) direc-
tion correctly predicts the widths of these dis-
tributions when added in quadrature to the track
errors discussed above, as shown by the curves
in Fig. 3. Consequently, the beam direction in the
Monte Carlo program has been perturbed by the
same amount.

Finally, to demonstrate that the Monte Carlo
simulation is in good agreement with the K_L data,
Figs. 4 and 5 show the lab momenta and opening
angle distributions for K_{l3} decays selected by the
requirement $(p'_0)^2 < -0.008$ GeV^2 (see part D). The
curves are the predicted shapes using the decay
parameters discussed below. The positive and
negative track momenta have been plotted sepa-
rately in Figs. 4(a) and 4(b), respectively, al-
though they are predicted to have the same shape
within the accuracy of our experiment. There are
no significant discrepancies between the data and
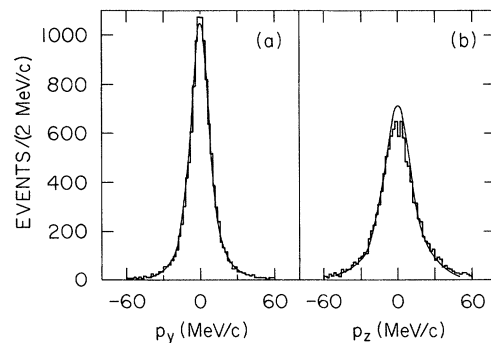the predictions for these variables or for any of

FIG. 2. Invariant mass of both charged tracks assum-
ing they are pions. Neither the K_L decay requirement
nor the K_S mass cut has been imposed on the data. The
curve is the prediction of the Monte Carlo simulation for
K_S decays.

FIG. 3. The components of the missing transverse
momentum for events of the type $K_L p \rightarrow K^\pm \pi^\mp p$: (a) par-
allel to film plane, (b) perpendicular to film plane. The
curves show the expected widths of these distributions
from the track measurement errors plus a small un-
certainty in the beam direction.

the variables used in the subsequent analysis. Therefore, we can determine the decay parameters by comparing the data with the predictions of the Monte Carlo program, confident that it effectively simulates the experimental conditions.

D. Separation of Decay Modes

It is well known that the variable $(p_0')^2$ is useful for separating the $K_{\pi 3}$ decay mode from both K_{l3} modes.[7] This variable is defined as the K_L momentum squared in the frame where the π^0 momentum is transverse to the beam direction, assuming a $K_{\pi 3}$ decay (see Appendix). Neglecting resolution effects, $K_{\pi 3}$ decays are restricted to positive values of $(p_0')^2$, whereas K_{e3} and $K_{\mu 3}$ decays are concentrated at negative $(p_0')^2$ values. The $(p_0')^2$ distribution obtained in this experiment is shown in Fig. 6. The solid curve is the prediction of the Monte Carlo simulation using the parameters determined in the following sections. The K_{l3} background for $(p_0')^2 > 0$ comprises approximately 20% of the sharp $K_{\pi 3}$ peak, as shown by the dashed curve. The selection $(p_0')^2 < -0.008$ GeV^2 removes more than 99% of the $K_{\pi 3}$ decays but retains ~94% of the K_{l3} decays, leaving a sample of 15 800 unique K_{l3} decays.

Although it is possible to determine the $K_{\mu 3}^0/K_{e3}^0$ branching ratio by fitting the negative range of $(p_0')^2$ to the sum of the expected distributions for
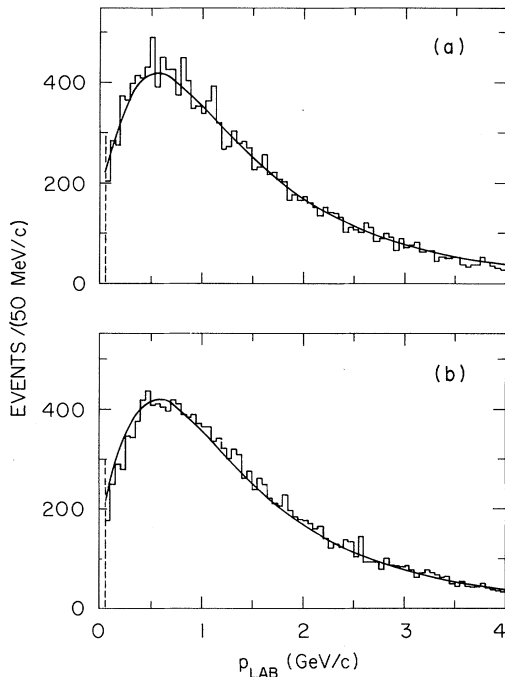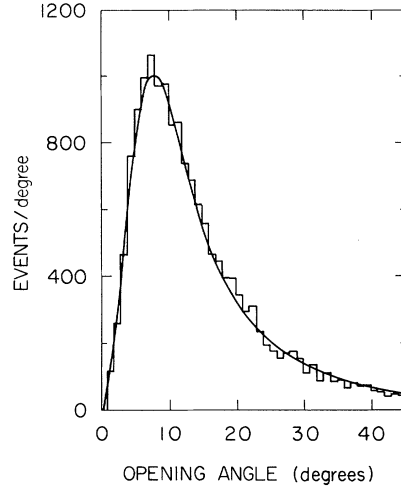
FIG. 5. The opening angle in the lab for K_{l3} decays selected by $(p_0')^2 < -0.008$ GeV^2. The curve is the prediction of the Monte Carlo simulation.

K_{e3} and $K_{\mu 3}$,[7] this procedure has two drawbacks. First, the $(p_0')^2$ distribution for K_{l3} decays is not independent of the beam spectrum. Thus any uncertainty in the indirect determination of the beam spectrum will be reflected in a fit to $(p_0')^2$. Second, $(p_0')^2$ does not provide a well-defined separation of the two K_{l3} modes. To circumvent these difficulties we define a new variable $(p_T')^2$, which depends only on the transverse momenta:

$$(p_T')^2 \equiv C_T^2 - p_T^2 \; ,$$

$$C_T \equiv m_K - (p_{1T}^2 + m_\pi^2)^{1/2} - (p_{2T}^2 + m_\mu^2)^{1/2}, \qquad (9)$$

$$p_{1T} > p_{2T} \; .$$

FIG. 4. The lab momentum of (a) positive and (b) negative tracks for K_{l3} decays selected by $(p_0')^2 < -0.008$ GeV^2. The curves are the predictions of the Monte Carlo simulation.
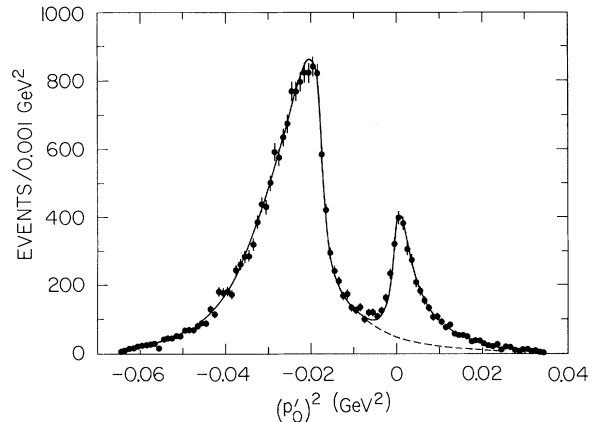
FIG. 6. $(p_0')^2$ distribution for entire K_L sample. The solid curve is the Monte Carlo prediction for the sum of all three decay modes, while the dashed curve is the sum of the K_{l3} modes alone for $(p_0')^2 > -0.008$ GeV^2.

Here p_T is the transverse momentum of the neutral particle (ν or π^0) and C_T is a cutoff depending on p_{1T} and p_{2T}, the transverse momenta of the two charged particles. Since there are no longitudinal momentum components in this definition, $(p'_T)^2$ is clearly independent of the beam momentum and has the useful property that $K_{\mu3}$ decays are restricted to positive values. To show this we write for a $K_{\mu3}$ decay in its rest frame

$$p^*_\nu = E^*_\nu = m_K - E^*_\pi - E^*_\mu$$

$$= m_K - (p^{*2}_\pi + m_\pi^2)^{1/2} - (p^{*2}_\mu + m_\mu^2)^{1/2} , \qquad (10)$$

from which it follows that

$$p_T \leqslant p^*_\nu$$

$$\leqslant m_K - (p_{\pi T}^2 + m_\pi^2)^{1/2} - (p_{\mu T}^2 + m_\mu^2)^{1/2}. \qquad (11)$$

Since it is not possible to distinguish the π from the μ, the larger permutation of the right-hand side of (11) is given by our definition of C_T in Eq. (9). Therefore, $(p'_T)^2 \geqslant 0$ for all $K_{\mu3}$ decays, neglecting experimental resolution. Since p_T can in general be larger in K_{e3} decays than in $K_{\mu3}$ decays, a region of unique K_{e3} decays exists for negative values of $(p'_T)^2$.

In Fig. 7 we show a scatter plot of $(p'_T)^2$ versus $(p'_0)^2$ to illustrate the relationship of these variables. The axes of this plot are seen to be kinematical boundaries for the $K_{\mu3}$ and $K_{\pi3}$ decay modes, while K_{e3} decays populate all regions of the plot. Selecting events with $(p'_T)^2 < -0.004$ GeV^2 results in a sample of 1871 K_{e3} decays, with less than 3% $K_{\mu3}$ contamination. The efficiency of this kinematical cut for selecting K_{e3} decays as a function of E^*_π and t is shown by the solid curve in Fig. 8(b), while

the pion energy spectrum is shown in Fig. 8(a). The efficiency varies gradually across the Dalitz plot and averages about 15% for all K_{e3} decays.

IV. DETERMINATION OF λ_+

As discussed in Sec. II, K_{e3} decays depend only on the f_+ form factor and not on f_-. To determine the parameter λ_+ in the linear expansion of f_+, we have used the unique K_{e3} events isolated as discussed above. In order to reduce contamination from the spillover of poorly measured $K_{\mu3}$ events to negative values of $(p'_T)^2$, we have accepted only those events with $(p'_T)^2 < -0.004$ GeV^2. The remaining $K_{\mu3}$ contamination ($< 3\%$) has been taken into account in the fits to the data.

The events selected in this manner are highly transverse, i.e., the decay plane is in general perpendicular to the beam direction in the K_L rest frame. Because of the large mass difference between the pion and the electron, the Lorentz transformation to the lab then has the interesting property that ~94% of the time the pion track has a higher lab momentum than the electron track. In addition, the transverse nature of the unique K_{e3} decays implies that $p^*_\pi \approx p_{\pi T}$, where p^*_π is the pion momentum in the K_L rest frame. Thus, the p_T distribution of the higher-momentum track in the
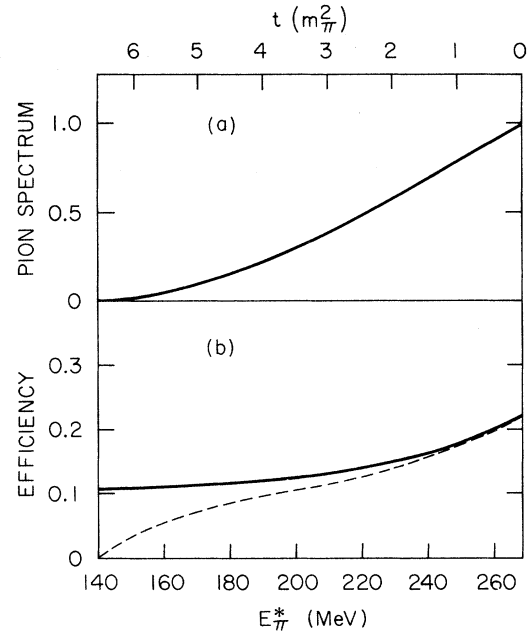
FIG. 8. (a) Dalitz plot energy spectrum of the pion in K_{e3} decays (for $\lambda_+ = 0.02$). (b) Solid curve shows the efficiency of the unique K_{e3} selection, i.e., the percentage of K_{e3} decays satisfying $(p'_T)^2 < -0.004$ GeV^2 and the cuts discussed in Sec. III B. Dashed curve shows the fraction of K_{e3} decays which satisfy the unique K_{e3} criteria and where the pion has a larger lab momentum than the electron.
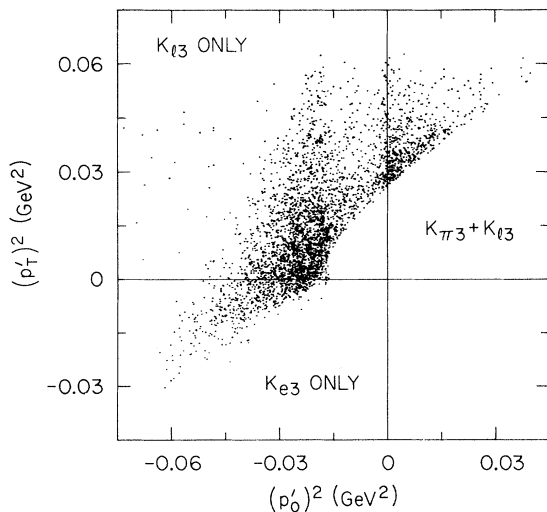

FIG. 7. Scatter plot of $(p'_T)^2$ versus $(p'_0)^2$, where $\sim\frac{1}{6}$ of the total K_L data are plotted. The decay modes which populate the various sectors are indicated.

lab is closely related to the p_π^* distribution and therefore to the t distribution [see Eq. (2)]. Identifying the pion in this manner is reliable for values of t smaller than about $5m_\pi^2$, but is inefficient for larger t. This can be seen from the dashed curve in Fig. 8(b), which shows the percentage of all K_{e3} decays which satisfy the unique K_{e3} selection criteria, and where $p_\pi > p_e$ in the lab.

The transverse-momentum (p_T) distribution of the higher-momentum track for the unique K_{e3} sample is shown in Fig. 9. To determine λ_+ we have fitted this distribution to the expression

$$Z(p_T) = f_+{}^2(0)\left[\langle A\rangle + 2\frac{\lambda_+}{m_\pi^2}\langle tA\rangle + \frac{\lambda_+{}^2}{m_\pi^4}\langle t^2A\rangle\right], \quad (12)$$

where the symbol $\langle\ \rangle$ indicates the Monte Carlo-generated distribution for p_T. A and t are functions of the Dalitz plot variables as defined in Eqs. (2) and (3). A least-squares fit has been performed in the interval $20 < p_T < 235$ MeV/c (solid curve in Fig. 9), yielding the result $\lambda_+ = 0.019 \pm 0.013$ with a χ^2 of 22 for 29 degrees of freedom (DF).[9]

The error on λ_+ is predominantly statistical with additional contributions from the uncertainties in the $K_{\mu3}$ contamination (0.004) and the Monte Carlo error parametrization (0.004). A fit to the more limited sample defined by $(p_T')^2 < -0.006$ GeV^2, where the $K_{\mu3}$ contamination is negligible, gave the same value for λ_+ indicating that the $K_{\mu3}$ background has been correctly treated. Since only transverse momenta are used in both the event selection and the λ_+ fit, the result is independent of the shape of the beam spectrum except for negligible momentum dependence of resolution effects. It is, however, sensitive to the K_{e3} radiative cor-

rections,[5] which modify the expected shape of the p_T distribution.[10]

V. DETERMINATION OF THE $K^0_{\mu3}/K^0_{e3}$ BRANCHING RATIO

We have determined the $K^0_{\mu3}/K^0_{e3}$ branching ratio (R) by fitting the experimental $(p_T')^2$ distribution to a sum of the expected distributions for K_{e3} and $K_{\mu3}$ decays. The data are shown in Fig. 10, where the $K_{\pi3}$ events have been removed by the requirement $(p_0')^2 < -0.008$ GeV^2. The dotted and dashed curves show the respective K_{e3} and $K_{\mu3}$ contributions, while the solid curve represents their sum. As discussed in Sec. III D, the fact that $K_{\mu3}$ decays are limited to the positive range of this variable makes it particularly sensitive to R.

In order to calculate the expected $(p_T')^2$ distributions it is necessary to assume values for λ_+ and $\xi(0)$. We take the value of λ_+ determined from our sample of unique K_{e3} events (see Sec. IV). The result we obtain for R is strongly dependent on the value assumed for λ_+, with a correlation $dR/d\lambda_+ \simeq -1.0$.[11] On the other hand, while the normalization of the $(p_T')^2$ distribution for $K_{\mu3}$ decays depends on $\xi(0)$, the shape of the distribution does not. Therefore, our result for R is insensitive to the value of $\xi(0)$ used in the simulation.

A fit of the $(p_T')^2$ distribution in the range $-0.022 < (p_T')^2 < 0.054$ GeV^2 is shown by the curve on Fig. 10. This fit yields an uncorrected ratio $R = 0.758 \pm 0.038$ with a χ^2 of 101 for 74 DF. The error is the statistical error multiplied by the factor $(\chi^2/\text{DF})^{1/2}$ to account for possible systematic errors in the data.[12]

To obtain a final ratio we have adjusted R by $-2 \pm 1\%$ to correct for K_{e3} decays which have un-
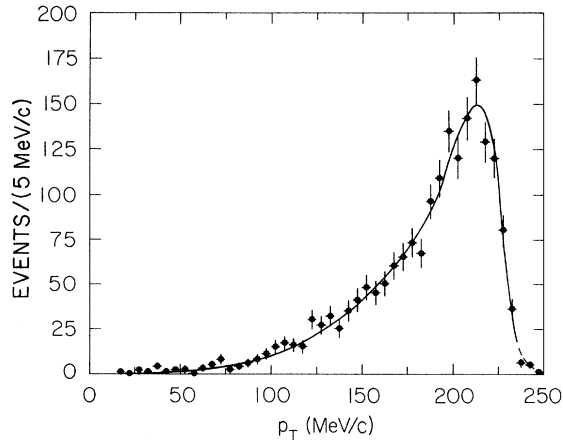
FIG. 9. Transverse momentum of the track with the larger lab momentum for the unique K_{e3} sample selected by $(p_T')^2 < -0.004$ GeV^2. The solid curve is the result of the λ_+ fit described in the text.
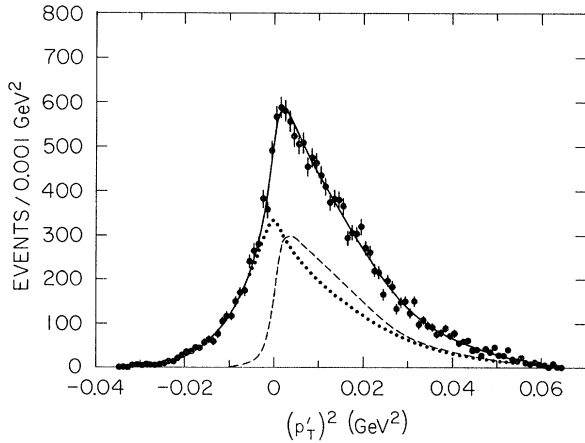
FIG. 10. $(p_T')^2$ distribution for the K_{l3} sample defined by $(p_0')^2 < -0.008$ GeV^2. The solid curve is the fitted sum of the K_{l3} decay modes, and the dotted and dashed curves show the respective K_{e3} and $K_{\mu3}$ components.
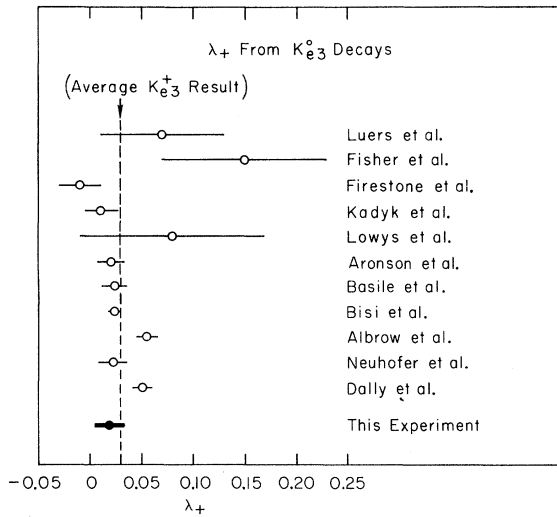
FIG. 11. Comparison of the present measurement of λ_+ with the results of previous K^0_{e3} experiments (Refs. 7, 13, 14). The dashed line is the average λ_+ obtained from charged K_{e3} decays (Ref. 1).
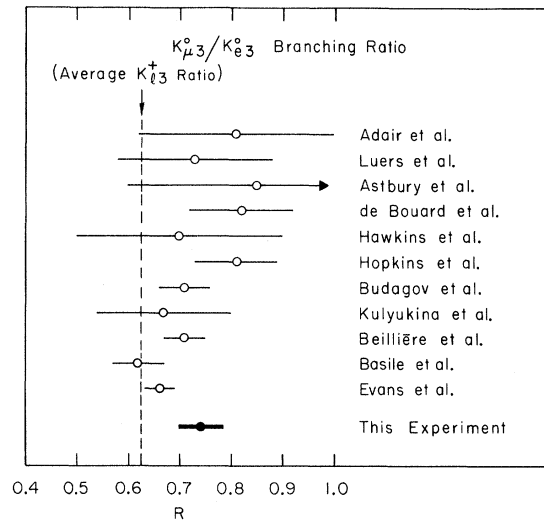

FIG. 12. Comparison of the $K^0_{\mu 3}/K^0_{e 3}$ branching ratio (R) obtained in this experiment with previous measurements (Refs. 7, 15). The dashed line is the average $K_{\mu 3}/K_{e 3}$ ratio from charged decays (Ref. 1).

measurable electron tracks due to large bremsstrahlung losses near the decay vertex. The following contributions have then been added in quadrature to the fitted error on R: 0.013 from the error in our determination of λ_+, 0.014 from the uncertainty in the Monte Carlo error parametrization, and 0.007 from the uncertainty in the bremsstrahlung correction. The final result is $R = 0.741 \pm 0.044$. As with λ_+, the dependence of R on the beam spectrum is negligible. However, the fitted value of R is sensitive to the radiative corrections,[5] which tend to shift K_{e3} events toward negative values of $(p'_T)^2$.[10]

VI. DISCUSSION OF K_{l3} FORM FACTORS

In this experiment we have measured both the parameter λ_+ and the $K^0_{\mu 3}/K^0_{e 3}$ branching ratio (R). Using the sample of unique K_{e3} decays we have obtained the value $\lambda_+ = 0.019 \pm 0.013$ for the slope of the f_+ form factor. This is shown in Fig. 11 together with previous measurements[7,13,14] and the average K^+_{e3} value[1] (dashed line). Our result is in agreement with the prediction of K^* dominance (0.023) and with the average charged K value. It is also compatible with previous K^0_{e3} measurements with the exception of the recent experiments of Albrow et al. and Dally et al.,[14] which find values approximately two standard deviations larger.

Our value for the branching ratio $R = 0.741 \pm 0.044$ has been determined by fitting the $(p'_T)^2$ distribution. This result is plotted in Fig. 12 along with the results of previous experiments[7,15] and the average ratio from charged K decays[1] (dashed line). Our ratio is larger than the more recent

measurements, but agrees with the trend of earlier measurements that the $K_{\mu 3}/K_{e 3}$ ratio is larger for neutral decays than for charged decays. This suggests that the $\Delta I = \frac{1}{2}$ rule, which predicts equal neutral and charged ratios, is not exactly satisfied by K_{l3} decays. Since the neutral and charged K results for λ_+ are compatible, the fact that R depends only on λ_+ and λ_0 [see Eq. (8)] implies that any breaking of the $\Delta I = \frac{1}{2}$ rule results from the f_0 form factor. This might be the consequence of the absence of a strong $I = \frac{1}{2}$ pole in the f_0 dispersion relation, which relates f_0 to the S-wave $K\pi$ system. The f_+ dispersion relation, on the other hand, is dominated by the $I = \frac{1}{2}K^*(890)$ in the P wave.

As discussed in Sec. V, our value for R is dependent on the value assumed for λ_+, with a correlation $dR/d\lambda_+ \simeq -1.0$. Our final ratio assumes $\lambda_+ = 0.019 \pm 0.013$, as determined from our data. We note that if λ_+ is assumed to be three standard deviations larger, the value obtained for R is still significantly higher than the previous results for both charged and neutral K decays.

Assuming μ-e universality, our results for λ_+ and R used in conjunction with Eqs. (5) and (8) yield the values $\xi(0) = 0.5 \pm 0.4$ and $\lambda_0 = 0.06 \pm 0.03$.[16] The correlation of these results with λ_+ is stronger for $\xi(0)$ ($d\xi(0)/d\lambda_+ \simeq -20$) than it is for λ_0 ($d\lambda_0/d\lambda_+ \simeq -0.6$). We note that our value for λ_0 is consistent with a linear rise of the f_0 form factor to the Callan-Treiman point, which would predict $\lambda_0 = 0.021$. Although most previous $K^0_{\mu 3}$ analyses have yielded negative values for $\xi(0)$ and λ_0,[1] the recent $K_{\mu 3}$ Dalitz plot analysis of Donaldson et al.[17] also

finds that f_0 is greater than $f_+(0)$ throughout the physical region and that f_0 extrapolates to the Callan-Treiman point.

VII. RESULTS ON $K_L \to \pi^+\pi^-\pi^0$

In this section we investigate our data on the $K_{\pi 3}$ decay mode, $K_L \to \pi^+\pi^-\pi^0$. These decays are concentrated at positive values of the variable $(p_0')^2$, as was discussed in Sec. III D. The experimental $(p_0')^2$ distribution is shown in Fig. 6. The dashed curve under the $K_{\pi 3}$ peak is the prediction of the Monte Carlo simulation for K_{l3} decays, assuming the decay parameters determined in the previous sections. It is seen that the leptonic decays comprise a large ($\sim 25\%$), but well-understood background to the $K_{\pi 3}$ decays.

In order to determine the branching ratio R_π of $K_L \to \pi^+\pi^-\pi^0$ to all charged K_L modes, we have fitted the $(p_0')^2$ distribution to a sum of the predicted distributions for the $K_{\pi 3}$ and K_{l3} modes. The simulated $K_{\pi 3}$ events have been generated assuming linear slope for the π^0 Dalitz plot energy distribution as described below, and have been weighted to correct for the Coulomb interaction of the charged pions.[6] Fitting the data in the interval $-0.060 < (p_0')^2 < 0.024$ GeV^2 gives the result $R_\pi = 0.146 \pm 0.004$. The fit, which is shown by the solid curve in Fig. 6, has a χ^2 of 115 for 82 DF.[12] The result has been adjusted slightly (-0.5%) to account for the loss of $K_{\pi 3}$ events with Dalitz pairs and of K_{e3} events due to large bremsstrahlung near the decay vertex (see Table I).

The error on R_π is the sum in quadrature of the statistical error multiplied by $(\chi^2/DF)^{1/2}$ and a contribution of 0.002 arising from the uncertainty in the parametrization of the measurement errors used in the simulation. The result is insensitive to the choice of the $E_{\pi^0}^*$ slope parameter, to the $K_{\pi 3}$ Coulomb corrections, and to the uncertainty in the shape of the beam spectrum. Also, variation of the K_{l3} decay parameters within several times their errors or omission of the K_{l3} radiative corrections does not significantly change the value of R_π.

Our result is significantly smaller than the World Average,[18] $R_\pi = 0.161 \pm 0.004$. As we believe that the K_{l3} background under the $K_{\pi 3}$ peak can be accurately predicted, such a discrepancy could only arise in our experiment from a loss of $K_{\pi 3}$ events at the scanning or measuring stage. However, in general we find that $K_{\pi 3}$ decays are easier to identify and measure than their leptonic counterparts. Furthermore, even if we assume that all $K_{\pi 3}$ events with Dalitz pairs were lost (we estimate that at least half are saved by careful scanning), R_π would be increased by less than a percent. We
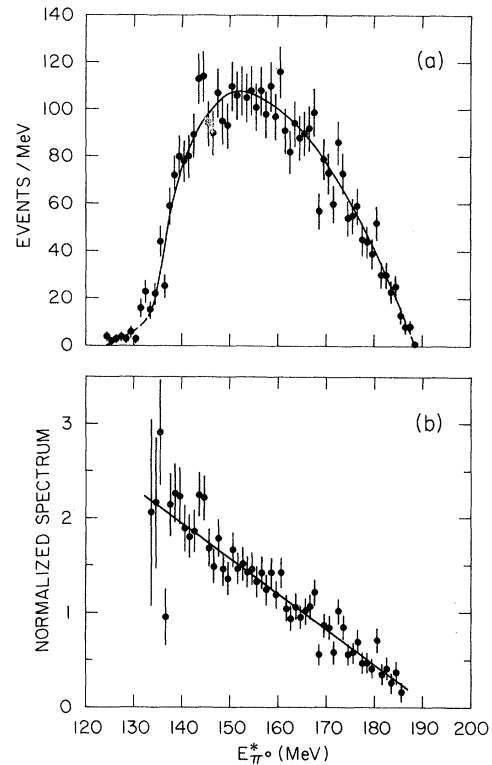

FIG. 13. (a) $E_{\pi^0}^*$ distribution for the $K_{\pi 3}$ sample defined by $(p_0')^2 > -0.005$ GeV^2. (b) Same data after subtraction of the expected K_{l3} background and division by Coulomb corrected $K_{\pi 3}$ phase space. The solid curves are the results of the $K_{\pi 3}$ matrix element fits described in the text.

do note that our measurement is based on approximately twice as many events as the best previous measurement.

As mentioned above, we have parametrized the deviation of the $K_{\pi 3}$ transition probability from pure phase space as[18]

$$W \propto 1 + g\frac{S_{12} - S_0}{m_\pi^2},$$

$$S_{12} = m_K^2 + m_\pi^2 - 2m_K E_{\pi^0}^*,$$

$$S_0 = \tfrac{1}{3}(m_K^2 + 3m_\pi^2),$$

(13)

where S_{12} is the mass squared of the two charged tracks taken as pions. We have determined the parameter g by fitting the $E_{\pi^0}^*$ distributions for the $K_{\pi 3}$ sample shown in Fig. 13(a), which is defined by $(p_0')^2 > -0.005$ GeV^2. This cut, which leaves 4051 events, retains approximately 98% of the $K_{\pi 3}$ events in the K_L sample, but minimizes the K_{l3} background at about 22%. The $E_{\pi^0}^*$ distribution is fitted to a sum of $K_{\pi 3}$ events generated according to both phase space and phase space multiplied by $E_{\pi^0}^*$, where the relative amounts are

given by Eq. (13). To this is added a K_{l3} background component which is fixed by our measurements of λ_+ and R, and which is normalized to the data with $(p'_0)^2 < - 0.008$ GeV^2. The best fit in the interval $133 < E^*_{\pi 0} < 186$ MeV, as shown by the solid curve in Fig. 13(a), resulted in the value $g = 0.73 \pm 0.04$, with a χ^2 of 66 for 51 DF. The error is the statistical error from the fit multiplied by $(\chi^2/\mathrm{DF})^{1/2}$.

To illustrate the linear nature of the $K_{\pi 3}$ matrix element squared, in Fig. 13(b) the $E^*_{\pi 0}$ distribution is plotted after subtraction of the expected K_{l3} background and division by $K_{\pi 3}$ phase space. A simple linear fit to this distribution yielded the same result as the fit described above, and is shown by the straight line. In both fits any quadratic dependence on $E^*_{\pi 0}$ was found to be negligible.[19]

If the four lowest $E^*_{\pi 0}$ points are eliminated from either fit the results are unchanged, but the χ^2 is decreased to 50 for 47 DF. The fitted value for g is also insensitive to the $K_{\pi 3}$ Coulomb corrections,[6] to the position of the $(p'_0)^2$ cut, and to the uncertainties in the Monte Carlo error parametrization. Furthermore, changing the values of R and R_π by several standard deviations, i.e., altering the amounts of $K_{e 3}$ and $K_{\mu 3}$ background, has no effect on g.

Our value, $g = 0.73 \pm 0.04$, differs significantly from the World Average,[18] $g = 0.60 \pm 0.03$. However, the recent high-statistics experiment of Messner et al.[20] has obtained the value $g = 0.659 \pm 0.004$, which is also significantly larger than the World Average. These results emphasize the failure of the $\Delta I = \frac{1}{2}$ rule for $K_{\pi 3}$ decays. This rule relates the values of g for the various charge modes of the $K_{\pi 3}$ decay, and predicts that $g = 0.47 \pm 0.01$ on the basis of charged $K_{\pi 3}$ results.[18]

VIII. CONCLUSIONS

In a high-statistics K_L experiment using a hydrogen bubble chamber we have measured the $K^0_{\mu 3}/K^0_{e 3}$ branching ratio (R) and the slope of the f_+ form factor (λ_+). The value we obtain for λ_+, 0.019 ± 0.013, is consistent with the predictions of K^* dominance and the $\Delta I = \frac{1}{2}$ rule. However, our branching ratio, $R = 0.741 \pm 0.044$, indicates a violation of the $\Delta I = \frac{1}{2}$ rule. Using our results for λ_+ and R we calculate $\lambda_0 = 0.06 \pm 0.03$, where λ_0 is the slope of the f_0 form factor. This number is consistent with a linear rise to the Callan-Treiman point. In addition, we have measured the branching ratio of $K_L \rightarrow \pi^+ \pi^- \pi^0$ to all charged K_L decay modes to be $R_\pi = 0.146 \pm 0.004$, and the $E^*_{\pi 0}$ slope of the $K^0_{\pi 3}$ matrix element squared to be $g = 0.73 \pm 0.04$. These latter results both differ significantly from previous measurements.

APPENDIX

In this appendix we discuss a slight modification to the definition of $(p'_0)^2$ which improves the separation of the $K_{\pi 3}$ and $K_{l 3}$ decay modes. This variable is normally defined as[7]

$$(p'_0)^2 = \frac{(m_K^2 - m_{\pi 0}^2 - m^2)^2 - 4 m_{\pi 0}^2 m^2 - 4 m_K^2 p_T^2}{4(p_T^2 + m^2)} ,$$

(A1)

where m is the effective mass of the two charged particles assuming they are pions, and p_T is the missing transverse momentum. This can be rewritten in the form

$$(p'_0)^2 = \frac{m_K^2}{p_T^2 + m^2}(p^{*2}_{\pi 0} - p_T^2) ,$$

(A2)

where $p^*_{\pi 0}$ is the momentum of the π^0 in the K_L rest frame, assuming a $K_{\pi 3}$ decay. In this form it is apparent that true $K_{\pi 3}$ decays are limited to positive values of $(p'_0)^2$, since p_T cannot exceed $p^*_{\pi 0}$. If we write

$$p^{*2}_{\pi 0} = E^{*2}_{\pi 0} - m_{\pi 0}^2$$

$$= \left(\frac{m_K^2 + m_{\pi 0}^2 - m^2}{2 m_K}\right)^2 - m_{\pi 0}^2 ,$$

(A3)

we see that when m exceeds its maximum value for a $K_{\pi 3}$ decay, $E^*_{\pi 0}$ is less than $m_{\pi 0}$ and $p^{*2}_{\pi 0}$ becomes negative. However, if m exceeds $m_K + m_{\pi 0}$, then $p^{*2}_{\pi 0}$ becomes positive again, even though $E^*_{\pi 0}$ is negative. Physically this situation corresponds to a $K_L \pi^0$ collision producing a $\pi^+ \pi^-$ pair. Actually, for our range of K_L beam momenta, $K_{e 3}$ decays can have large enough "dipion masses" to give positive values of $p^{*2}_{\pi 0}$ and $(p'_0)^2$. To avoid this possibility we have redefined $(p'_0)^2$ as

$$(p'_0)^2 = \frac{m_K^2}{p_T^2 + m^2}(E^*_{\pi 0}|E^*_{\pi 0}| - m_{\pi 0}^2 - p_T^2) ,$$

(A4)

which ensures that $K_{e 3}$ decays with increasingly large values of m will fall at increasingly negative values of $(p'_0)^2$. Both the data and the Monte Carlo

events have been plotted according to this prescription. The effect of this redefinition is to reduce the fraction of K_{e3} events with $(p_0')^2 > -0.008$ GeV^2 from ~13% to ~4%, thereby decreasing the background under the $K_{\pi3}$ peak. The $(p_0')^2$ distributions for $K_{\mu3}$ and $K_{\pi3}$, however, are left unchanged by the new definition. We note that the same effect can be achieved by using only those events with $m < m_K$ when plotting $(p_0')^2$.

In a similar fashion, the variable $(p_T')^2$ defined in Sec. III D, has been computed as $C_T |C_T| - p_T^2$. It is possible for K_{e3} decays with large pion and electron transverse momenta to give negative values of C_T, and the above definition ensures that they will be identified as unique K_{e3} decays with $(p_T')^2 < 0$. However, the number of such events is very small (~20) and our results are not affected by this modification.

*Work supported by the U. S. Atomic Energy Commission.

†Present Address: Duke University, Durham, North Carolina.

‡Present Address: Lawrence Berkeley Laboratory, Berkeley, California.

§Present Address: Purdue University, Lafayette, Indiana.

[1] M. K. Gaillard and L.-M. Chounet, CERN Report No. CERN 70-14, 1970 (unpublished); L.-M. Chounet, J.-M. Gaillard, and M. K. Gaillard, Phys. Rep. **4C**, 199 (1972).

[2] G. W. Brandenburg, A. D. Brody, W. B. Johnson, D. W. G. S. Leith, J. S. Loos, G. J. Luste, J. A. J. Matthews, K. Moriyasu, B. C. Shen, W. M. Smart, F. C. Winkelmann, and R. J. Yamartino, Phys. Rev. D **7**, 708 (1973).

[3] From a rescan of a fraction of the film the scanning efficiency for unassociated 2-prong events was determined to be $(93 \pm 1)\%$. The only events excluded from the unassociated 2-prong category were obvious electron pairs (~0° opening angle in all views and a low-momentum track). We estimate that $<0.1\%$ of the K_L decays were lost by this criterion.

[4] F. T. Solmitz, A. D. Johnson, and T. B. Day, LRL Group A Programming Report No. P-117, 1966 (unpublished).

[5] E. S. Ginsberg, Phys. Rev. **171**, 1675 (1968); E. S. Ginsberg, *ibid.* **174**, 2169 (1968); E. S. Ginsberg, Phys. Rev. D **1**, 229 (1970).

[6] A. Neveu and J. Scherk, Phys. Lett. **27B**, 384 (1968).

[7] D. Luers, I. S. Mittra, W. J. Willis, and S. S. Yamamoto, Phys. Rev. **133**, B1276 (1964); H. W. K. Hopkins, T. C. Bacon, and F. R. Eisler, Phys. Rev. Lett. **19**, 185 (1967); P. Basile, J. W. Cronin, B. Thevent, R. Turlay, S. Zylberajch, and A. Zylbersztejn, Phys. Rev. D **2**, 78 (1970).

[8] Our data cannot distinguish between a linear and a quadratic t dependence for f_+. If a quadratic term $\lambda_+' t^2/m_\pi^4$ is added to the linear expansion of f_+, the fit allows all reasonable values of λ_+ and λ_+' which satisfy the empirical relation $\lambda_+ + 4\lambda_+' \simeq 0.02$. Equivalently, we have measured the slope of f_+ at an average t of about $2m_\pi^2$.

[9] The data points for $20 < p_T < 100$ MeV/c have been grouped into four bins for the fit: 20–60, 60–80, 80–90, 90–100 MeV/c.

[10] Fits to the data have also been made assuming no radiative corrections to the K_{l3} matrix elements. These yielded the value $\lambda_+ = 0.027 \pm 0.014$ and the corrected ratio $R = 0.705 \pm 0.044$, however in both cases the χ^2 of

the fit was unchanged.

[11] If quadratic expansion of f_+ is assumed, our result for R is independent of small changes in λ_+ and λ_+' which leave the combination $\lambda_+ + 4\lambda_+'$ constant (see Ref. 8).

[12] By determining R and R_π for more restricted ranges of the variables $(p_T')^2$ and $(p_0')^2$, respectively (e.g., between -0.02 and $+0.02$ GeV^2), the χ^2/DF of the fits can be reduced without affecting the results or their accuracy. On the other hand, the extent to which systematic effects are understood is demonstrated by fitting the entire ranges of these variables, and the fitted errors are then scaled by the factor $(\chi^2/\text{DF})^{1/2}$ to account for such uncertainties.

[13] G. P. Fisher *et al.*, ANL Report No. 7130, 1965 (unpublished); A. Firestone *et al.*, Phys. Rev. Lett. **18**, 176 (1967); J. A. Kadyk *et al.*, *ibid.* **19**, 597 (1967); J. P. Lowys *et al.*, Phys. Lett. **24B**, 75 (1967); H. Aronson *et al.*, Phys. Rev. Lett. **20**, 287 (1968); P. Basile *et al.*, Phys. Lett. **26B**, 542 (1968); V. Bisi *et al.*, *ibid.* **36B**, 533 (1971); G. Neuhofer *et al.*, *ibid.* **41B**, 642 (1972).

[14] M. G. Albrow, D. Aston, D. P. Barber, L. Bird, R. J. Ellison, C. H. Halliwell, R. E. H. Jones, A. D. Kanaris, F. K. Loebinger, P. G. Murphy, M. G. Strong, J. Walters, D. D. Yovanovich, and R. F. Templeman, in *Proceedings of the XVI International Conference on High Energy Physics, Chicago-Batavia, Ill., 1972,* edited by J. D. Jackson and A. Roberts (NAL, Batavia, Ill., 1973) Vol. 2, p. 209; E. Dally, P. Innocenti, E. Seppi, C.-Y. Chien, B. Cox, L. Ettlinger, L. Resvanis, R. A. Zdanis, C. D. Buchanan, D. J. Drickey, F. D. Rudnick, P. F. Shepard, D. H. Stork, H. K. Ticho, Phys. Lett. **41B**, 647 (1972).

[15] R. K. Adair *et al.*, Phys. Lett. **12**, 67 (1964); P. Astbury *et al.*, *ibid.* **16**, 80 (1965); X. deBouard *et al.*, Nuovo Cimento **52A**, 662 (1967); C. J. B. Hawkins, Phys. Rev. **156**, 1444 (1967); I. A. Budagov *et al.*, Nuovo Cimento **57**, 182 (1968); L. A. Kulyukina *et al.*, Zh. Eksp. Teor. Fiz. **53**, 29 (1967) [Sov. Phys.—JETP **26**, 20 (1968)]; P. Beillière *et al.*, Phys. Lett. **30B**, 202 (1969); G. R. Evans *et al.*, Phys. Rev. D **7**, 36 (1973).

[16] We have chosen that solution of the quadratic expression for $\xi(0)$ in Eq. (5) and for λ_0 in Eq. (8) which is smaller in magnitude. Furthermore, we have neglected the radiative corrections to these equations (see Ref. 5), which change the results by less than a percent.

[17] G. Donaldson, D. Fryberger, D. Hitlin, J. Liu, B. Meyer, R. Piccioni, A. Rothenberg, D.Uggla, S. Wojcicki, and D. Dorfan, Phys. Rev. Lett. **31**, 337 (1973).

[18] Particle Data Group, Rev. Mod. Phys. **45**, S1 (1973).

[19]If a term $h(S_{12} - S_0)^2/m_\pi^4$ is added to Eq. (13), the $E^*_{\pi 0}$ fits yield $h = 0.01 \pm 0.06$ with no change in g or in the χ^2.

[20]R. Messner, A. Franklin, R. Morse, U. Nauenberg, D. Dorfan, D. Hitlin, J. Liu, and R. Piccioni, in

Proceedings of the XVI International Conference on High Energy Physics, Chicago-Batavia, 1972, edited by J. D. Jackson and A. Roberts (NAL, Batavia, Ill., 1973) Vol. 2, p. 209. These authors find that a quadratic term is necessary to fit the $E^*_{\pi 0}$ distribution.

Search for Rare K^+ Decays. I. $K^+ \to \mu^+ \nu \bar{\nu} \nu$*[†]

C. Y. Pang and R. H. Hildebrand

Enrico Fermi Institute and Department of Physics, The University of Chicago, Chicago, Illinois 60637

G. D. Cable

Enrico Fermi Institute, The University of Chicago
and Department of Physics, The University of Arizona, Tucson, Arizona 85721

R. Stiening[‡]

Lawrence Berkeley Laboratory, Berkeley, California 94720
(Received 14 May 1973)

In a counter experiment at the LBL Bevatron, we have searched for the process $K^+ \to \mu^+ \nu \bar{\nu} \nu$ and have found no evidence for its existence. We have recorded ten events which could be examples of this decay mode, but could also be examples of $K^+ \to \mu^+ \nu \gamma$ in which the γ was not detected. Treating these as unidentified events and assuming the μ^+ spectrum proposed by Bardin, Bilenky, and Pontecorvo, we obtain a decay rate $\Gamma(K^+ \to \mu^+ \nu \bar{\nu} \nu) \leq 6 \times 10^{-6} \Gamma(K^+ \to \text{all})$ (90% confidence level). The data are presented in such a way as to allow calculation of rates for any assumed spectrum. The experiment provides a test for higher-order weak processes and sets constraints on certain first-order models.

I. INTRODUCTION

A. Experiments on Two K^+ Decay Modes

In this and a following paper we report on concurrent experiments to search for the K^+ decay modes $K^+ \to \mu^+ \nu \bar{\nu} \nu$ (I) and $K^+ \to \pi^+ \nu \bar{\nu}$ (II). Since the apparatus was common to the two experiments, its description in I will serve both papers.

B. The Decay $K^+ \to \mu^+ \nu \bar{\nu} \nu$

In an earlier publication[1] we have given preliminary results of a search for the decay process $K^+ \to \mu^+ \nu \bar{\nu} \nu$. We now present final results and give a detailed account of the work.

The well-known current-current theory of weak interactions appears to give an adequate description of all observed weak processes. This theory leads to divergences, however, when applied to certain high-order interactions, and at very high energies it leads to the violation of unitarity.[2]

The decay process

$$K^+ \to \mu^+ \nu \bar{\nu} \nu \tag{1}$$

cannot occur in the first order of the conventional theory. The experimental investigation of this process may therefore give information about the structure of higher-order weak effects. Furthermore, since this decay process involves an extraordinary number of fermions, neutrinos in particular, its investigation provides information on two proposed first-order effects: (1) a neutrino-neutrino interaction other than the usual weak interaction (such an interaction could be very strong without having been seen[3]), and (2) a six-fermion interaction[4,5] in addition to the ordinary (four-fermion) weak interaction.

For K's decaying at rest, process (1) should be uniquely distinguished from all known decays by the emission of μ's in the energy interval $60 < T_\mu < 100$ MeV unaccompanied by other charged particles or by γ's. In this experiment, K's from the LBL Bevatron were brought to rest in a carbon stopper. The K's and their decay products were detected by an array of scintillation and Čerenkov counters. The μ's were identified by their μ-e decays; the μ energies were determined by range. In order to reject background events from pro-